reversed, the opposite is true and the sign of n has to be changed in the above equations. These two cases can easily be distinguished for $N > 4$ by comparing $A_1^{((2))}$ and $A_1^{((-2))}$, but the ambiguity remains for $N = 4$. Alternatively, this ambiguity can be resolved using tilt-induced shift measurements [15,16], which additionally determine the sign of τ_0. The measurements of $|\tau_0|$ and C_3 cannot be separated and hence C_3 can only be measured when the tilt coil strength is calibrated accurately. Alternatively, if C_3 is known independently, $|\tau_0|$ can be determined with all the other parameters.

Full expressions for the accuracy of the determined parameters in terms of the accuracies σ_C and σ_A of the estimates for C_1 and A_1 are given in Table 2.

For overdetermined datasets, the RMS difference between the experimental values $C_1^{(n)}$, $A_1^{(n)}$ and the equivalent values predicted according to Eqs. (4) and (5) from the fitted parameters is a measure of the quality of the fit.

With lower symmetry dataset geometries, the full set of aberration parameters must be determined from the measured C_1 and A_1 values using a least-squares fit as previously described [17].

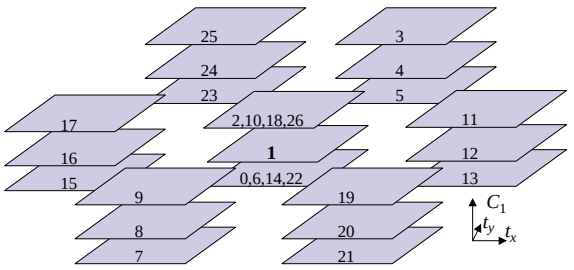

Fig. 1. Schematic illustration of a combined defocus/tilt azimuth dataset with images numbered in recording sequence. A three-member focal series is recorded for each of six different tilt azimuth angles and also for axial illumination. Additional axial images are recorded between each pair of tilted datasets with the focus level unchanged, allowing measurement of the focus drift during acquisition. The order in which the images are recorded (indicated by numbers 0…26) was chosen to minimize the influence of focus drift and lens and deflector hysteresis by ensuring that focus and tilt are not changed simultaneously and by recording series with opposite tilts in immediate succession.

2.1. Systematic errors in the PCI due to noise

In very short focus series of images with large beam tilts, the astigmatism determination algorithm [7] occasionally fails to find the global maximum in the F_{PCI} and instead, a local maximum with a small value of A_1 is found. This arises because noise in the images also contributes to the conjugate antisymmetry measured by the PCI and for the initial trial value $A_1 = 0$, gives rise to a false, weak circular ring pattern in the f_{PCI} in addition to the true strongly elliptical ring pattern, leading to spurious maxima in the F_{PCI}. However, this artefact can easily be avoided by starting from a nonzero A_1 trial value or by choosing unequal and sufficiently large focus steps.

More formally, using the notation of [7], the restoration filters

$$r_i' = r_i e^{i\gamma_s(C_1,A_1)} \tag{20}$$

(1) Register images 0 and 2 with image 1 using phase-compensated PCFs.	
(2) Restore image wave in plane of image 1.	
(3) For all other axial images	(a) Register image to current restoration using the PCF with predicted images.
	(b) Add image to restoration
(4) Determine absolute focus and 2-fold astigmatism using the PCI.	
(5) For all tilted focus series.	(a) Coarsely register the position of the central tilted image
	(b) Register first and last image to middle image using PCFs.
	(c) Restore aberrated wavefunction from the three tilted images.
	(d) Determine apparent absolute defocus and astigmatism using the PCI.
At this point, the apparent absolute defoci C_{1n} and astigmatisms A_{1n} ($n \in \{0\ldots26\}$) of all images are known.	
(7) Determine drift-corrected aberrations for the tilted sets ($n \in \{0\ldots5\}$) as $A_1^{(n)} = A_{1(4n+4)}$ and $C_1^{(n)} = C_{11} + (C_{1(4n+3)} + C_{1(4n+5)} - C_{1(4n+2)} - C_{1(4n+6)})/2$.	
(8) Determine the antisymmetric aberrations, including the beam tilt for the axial images and the magnitude and direction of the injected tilt, analytically or numerically.	
(9) Re-calculate the restoration from the axial images	
(10) For all tilted focus series.	(a) Calculate restoration from tilted images with beam tilt corrected.
	(b) Register with restoration from axial images using PCF.
(11) Calculate the restoration from all images	

Fig. 2. Procedure for the determination of all aberration coefficients (steps (1)–(8)) and subsequent tilt series restoration (steps (9)–(11)) from a tilt/focus dataset with six tilt azimuths. The image numbers refer to the dataset geometry shown in Fig. 1.